A Detailed Model for Multi-Energy Systems with Integrated Control Schemes

Styliani A. Vomva
Dept. of Electr. & Comput. Eng.
Aristotle University of Thessaloniki
Thessaloniki, Greece
stylianav@ece.auth.gr

Anthi S. Papadopoulou
Dept. of Electr. & Comput. Eng.
Aristotle University of Thessaloniki
Thessaloniki, Greece
anthipapado@ece.auth.gr

Georgios C. Kryonidis
Dept. of Electr. & Comput. Eng.
Aristotle University of Thessaloniki
Thessaloniki, Greece
kryonidi@ece.auth.gr

Angelos I. Nousdilis
Dept. of Electr. & Comput. Eng.
University of Western Macedonia
Koila, Greece
a.nousdilis@uowm.gr

Georgios C. Christoforidis
Dept. of Electr. & Comput. Eng.
University of Western Macedonia
Koila, Greece
gchristoforidis@uowm.gr

Grigoris K. Papagiannis
Dept. of Electr. & Comput. Eng.
Aristotle University of Thessaloniki
Thessaloniki, Greece
gpapagia@ece.auth.gr

***Abstract*—Considering the residential sector, greenhouse gas emissions can be effectively reduced by the widespread deployment of distributed renewable energy sources (DRESs) in low-voltage (LV) electrical networks (ENs). Through the electrification and the integration of different energy systems, the exploitation of the locally generated renewable energy can be further increased, acting also as an efficient countermeasure to the technical challenges posed by the intermittent nature of DRES units. This work deals with the modeling of multi-energy systems (MESs) consisting of ENs and district heating networks (DHNs). A detailed model is developed and compared with an already existing open-source tool in terms of accuracy and modeling capability. The model is enhanced by the incorporation of thermal droop control schemes into the DHN components. The validity of the proposed model is assessed via simulations on a MES composed of a LV EN and a real DHN, highlighting also the contribution of the integrated control schemes towards improving the operational reliability and exploitation of the DRES potential.**

***Index Terms*—District heating network, droop control, electrical network, integrated operation, integrated modeling.**

I. Introduction

A. Motivation and Background

The European Union (EU) has clearly set the path for promoting renewable energy sources (RESs) to cover the 40 % of the gross final energy consumption till 2030 [1], respecting the worldwide efforts towards greenhouse gas emissions minimization. This can be attained by proliferating the RES integration in the electrical networks (ENs) and especially in distribution grids by means of distributed RESs (DRESs).

In parallel to the DRES promotion, the electrification in end-use sectors is also proposed by the EU [2]. A promising solution to achieve this objective is the effective integration of different energy systems [3], that has been already supported by the EU [4]. Thus, the formulation of the so-called multi-energy systems (MESs) is recommended [5], where the various energy systems are coupled to cover the energy demand in a collaborative and efficient way. Besides, the MES concept introduces additional operational flexibility due to the controllable energy exchange among the different energy systems, thus contributing to the mitigation of the technical challenges that can arise by the high DRES penetration in ENs [6]. Among them, a severe issue is the violation of voltage limits, jeopardizing the reliable operation of the ENs [7].

Within the various types of MES in the residential sector, the combined operation of low-voltage (LV) distribution ENs and district heating networks (DHNs) seems to be more common, since it is driven by the electrification of the thermal loads [8]. It is evident that an appropriate modeling approach is needed to evaluate the integrated operation of MESs.

B. Relevant Literature

To properly model MESs, the concept of the energy hub was initially proposed in [9], where the inputs and outputs of the whole system are interconnected via a coupling matrix consisting of the conversion and the storage devices characteristics. Nevertheless, this modeling approach does not focus on the detailed network operation.

An improved MES modeling is introduced in [10], where the EN and DHN characteristics are taken into consideration. However, the literature lacks of a common-established solution for modeling DHNs, due to their complicated nature. Specifically, the network characteristics, temperature at the thermal nodes, mass flow within the pipes, etc., can be treated as constants or variables, depending on the adopted assumptions [11]. To facilitate the modeling of the DHN, an equivalent of electrical power system model is proposed in [12]. Moreover, a component-oriented modeling approach is presented in [13], describing the way each DHN component contributes to the heat medium circulation. The integrated operation of ENs and DHNs is investigated in [14], where an equivalent model of the DHN is employed to tackle the inherent modeling difficulties of DHNs.

As a common drawback, all the above-mentioned modeling approaches do not consider the integration of control strategies in the components of both ENs and DHNs while analyzing the network operation. In [15], heat pumps (HPs) are controlled to respond to ENs demand-side management programs, while in [16], the droop control is introduced to the operation of DHNs, and more specifically to the thermal storage units. However, the effect of the proposed controls on the operation of the ENs and DHNs is not considered, since the accurate modeling of both the networks is missing. An initial attempt was made in [17], where the

Citation information, DOI: 10.1109/SEST57387.2023.10257325

integrated operation of ENs and DHNs is enhanced by the implementation of droop control schemes for the PVs. The model lacks the use of control strategy dedicated to the HPs, while its efficiency comes at the loss of green energy due to active power curtailment of the PVs generation.

C. Contributions

In this paper, a detailed model for the steady-state, balanced operation of integrated ENs and DHNs is developed. The main contribution is the introduction of a thermal droop control scheme (TDCS) aiming at controlling the temperature across the DHN. Note that this control scheme is proposed for the first time in the literature. Additional strengths of this work involve:

- A comparative analysis with open-source software packages *pandapower* [18] and *pandapipes* [19] to evaluate the accuracy of the developed model.
- The efficacy of the integrated operation of ENs and DHNs to mitigate overvoltages without DRES active power curtailment.

Simulations are conducted on a MES composed of a LV EN and a real DHN to evaluate the performance of the proposed approach and assess the impact of the TDCS on the reliable operation of both EN and DHN.

II. Mathematical Formulation

The proposed modeling approach is based on the equations describing EN and DHN, along with the coupling device employed to achieve their integrated operation.

A. Electrical Network

For the mathematical description of an EN consisting of Ξ nodes, the well-known power flow equations are given by:

$$P_i = \sum_{j=1}^{\Xi} V_i V_j Y_{ij} cos(\delta_j - \delta_i + \gamma_{ij}), \quad \forall i \in \Xi \tag{1}$$

$$Q_i = -\sum_{j=1}^{\Xi} V_i V_j Y_{ij} sin(\delta_j - \delta_i + \gamma_{ij}), \quad \forall i \in \Xi \tag{2}$$

Here, P_i and Q_i stand for the active and reactive power absorption at the i-th node of the EN, while V_i and δ_i correspond to the magnitude and angle of the voltage at the same node, respectively. Y_{ij} and γ_{ij} represent the magnitude and the angle of the admittance of the line connecting i-th and j-th nodes.

B. District Heating Network

Within a DHN, the heat medium flows from a primary source to the loads through the set of pipes comprising the supply subsystem. The heat medium returns to the main source through another set of pipes corresponding to the return subsystem. Due to the temperature variation propagation, transport delay is introduced in both subsystems and the heat medium needs time to travel from the beginning towards the end of a pipe. Contrary to ENs, this time delay may reach minutes or hours depending on the velocity of the heat medium and various pipe parameters until reaching to a new steady-state condition. For analyses in time with time-step longer than the transport delay, this phenomenon can be neglected. In this work, single time-step analysis is implemented; thus, no delay in the thermal propagation is considered.

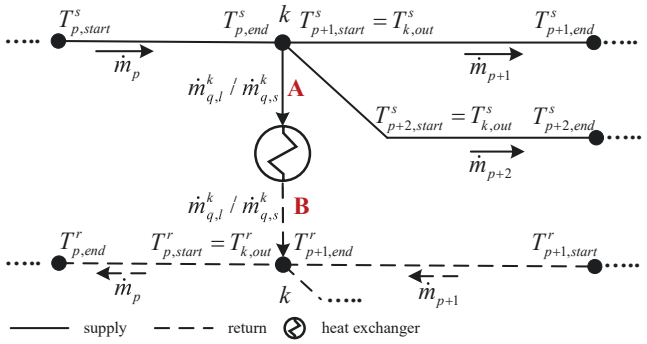

Fig. 1. Generic configuration of a DHN.

Thermal sources can be either centrally located at a single node or distributed in several nodes of the network. The supply subsystem is physically connected to the return subsystem through heat exchangers that model thermal loads or sources.

To fully describe the operation of a DHN, both an hydraulic and a thermal model are necessary. The hydraulic model deals with the mass flow within the pipes and the heat exchangers, while the thermal model aims at calculating the temperature at several points of the supply and the return subsystems. In this paper, a generic modeling approach is adopted where variable mass flows and temperatures are assumed (VF-VT scheme) [11]. Additionally, the combined modeling approach of [10] is adopted.

In Fig. 1, a general structure of pipes and nodes connected via a heat exchanger, either load or source, is presented. The mass flow through the p-th pipe is denoted as $\dot{m}_p$, while the nodal mass flow of the thermal load and source connected to node k are represented by $\dot{m}^k_{q,l}$, and $\dot{m}^k_{q,s}$, respectively. Negative value of the nodal mass flow indicates source connection, i.e., the heat medium flows from the return to the supply subsystem. The mass flow within a certain pipe in the supply subsystem is assumed to be the same with the corresponding pipe in the return subsystem. Moreover, the mass flow within a load/source is assumed to be the same for both the supply and the return subsystems. $T^x_{p,start}$ and $T^x_{p,end}$ stand for the temperature in the sending and receiving end of the p-th pipe, respectively. Superscript $x \in \{s, r\}$ denotes the examined subsystem, namely supply (s) and return (r). $T^x_{k,out}$ is the temperature of the heat medium leaving k-th node in the subsystem x.

The temperature of the heating medium leaving a load/source before mixing within the return/supply subsystem, respectively, is assumed to be an *a priori* known parameter. $T^k_{o,l}$ and $T^k_{o,s}$ stand for the outlet temperature of the load and source, respectively. The temperature of the heat medium in points A and B depends on whether this heat exchanger is a load or source. In case of a load, these temperatures are equal to $T^s_{k,out}$ and $T^k_{o,l}$. On the contrary, $T^k_{o,s}$ and $T^r_{k,out}$ are the corresponding temperatures in case of a thermal source.

The hydraulic model is based on the following principles:

- Continuity of mass flow in each node as expressed by (3). The set of equations corresponding to all network nodes are defined in (4).

$$\sum_{p \in I_k} \dot{m}_p - \sum_{p \in O_k} \dot{m}_p = \dot{m}^k_{q,l} + \dot{m}^k_{q,s}, \quad \forall k \in \Omega \tag{3}$$

$$\mathbf{A} \cdot \dot{\mathbf{m}} = \dot{\mathbf{m}}_{\mathbf{q,l}} + \dot{\mathbf{m}}_{\mathbf{q,s}} \tag{4}$$

Here, Ω is the set of DHN nodes, I_k is the set of pipes where the flow comes into node k and the O_k is the set

of pipes where the heat medium leaves the node k. $\mathbf{A}$ is the incidence matrix containing information related to the network topology [10], $\dot{\mathbf{m}}$ is the vector of the mass flow of the network pipes, while $\dot{\mathbf{m}}_{\mathbf{q,l}}$ and $\dot{\mathbf{m}}_{\mathbf{q,s}}$ correspond to the vectors of the nodal mass flow of loads and sources, respectively.

- Zero loop pressure. In every loop within a DHN, the sum of pressure deviations due to friction must be equal to zero. This is mathematically expressed as follows:

$$\mathbf{B} \cdot \mathbf{h} = \mathbf{0} \tag{5}$$

where $\mathbf{B}$ and $\mathbf{h}$ correspond to the loop incidence matrix relating loops to branches, and the vector of pressure deviations, respectively [10].

With regards to the thermal model, the following equations are used:

- Eq. (6) is introduced to model the temperature drop across each pipe due to the thermal losses caused by the thermal conductivity between the pipe and the ground.
- Eqs. (7a) and (7b) are employed to model the mixing of the heating medium in the supply and return subsystems, respectively. After the temperature mixing, the temperature leaving a node is the same in the beginning of all the connected pipes and loads/sources.
- Eqs. (8a) and (8b) describe the heat exchanger model for loads and sources, respectively.

$$T_{p,end} = (T_{p,start} - T_a) \cdot e^{-\frac{\lambda_p L_p}{c_p \dot{m}_p}} + T_a, \quad \forall p \in \Pi \tag{6}$$

$$T_{k,out} \cdot \Big(\sum_{p \in O_k} \dot{m}_p + \dot{m}^k_{q,l}\Big) = \\ = \sum_{p \in I_k} (\dot{m}_p \cdot T_{p,end}) - \dot{m}^k_{q,s} \cdot T^k_{o,s}, \quad \forall k \in \Omega \tag{7a}$$

$$T_{k,out} \cdot \Big(\sum_{p \in O_k} \dot{m}_p - \dot{m}^k_{q,s}\Big) = \\ = \sum_{p \in I_k} (\dot{m}_p \cdot T_{p,end}) + \dot{m}^k_{q,l} \cdot T^k_{o,l}, \quad \forall k \in \Omega \tag{7b}$$

$$Q_{k,l} = c_p \dot{m}^k_{q,l} (T^s_{k,out} - T^k_{o,l}), \quad \forall k \in \Phi \tag{8a}$$

$$Q_{k,s} = c_p \dot{m}^k_{q,s} (T^k_{o,s} - T^r_{k,out}), \quad \forall k \in \Theta \tag{8b}$$

Here, Π, Φ, and Θ are the set of pipes, loads, and sources in the DHN. λ_p and L_p stand for the heat transfer coefficient per unit length and the length of the p-th pipe, respectively. $Q_{k,l}$ and $Q_{k,s}$ express the thermal power of the load and source connected to the k-th node, respectively. Finally, c_p is the specific heat capacity of the heat medium, while T_a is the temperature of the ground where the pipes are installed.

C. Coupling Device and Proposed Control Scheme

Among the various technologies that can be used to generate heat via the Power-to-Heat technology, HPs are selected. Their distinct characteristic is the unidirectional energy flow from ENs to DHNs. The mathematical expression that relates the input with the output of a HP is expressed as follows:

$$P^{el}_{hp,i} = Q_{hp,k}/COP \tag{9}$$

Here, $P^{el}_{hp,i}$ stands for the electrical consumption of the HP installed in the i-th EN node. $Q_{hp,k}$ is the thermal power generated by the HP installed in the k-th DHN node, which corresponds to $Q_{k,s}$. COP represents the HP coefficient of performance.

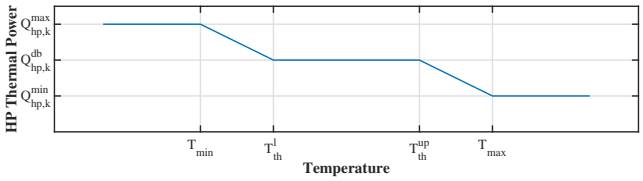

Fig. 2. Proposed TDCS.

The thermal power output of the HPs may lead to uncontrollable increase of the temperature in the supply subsystem of a DHN. To regulate temperature and maintain it within the acceptable limits, a TDCS can be incorporated into HPs operation, as in [16] used for the thermal storage. The main scope is to actively control temperature and indirectly share the thermal generation among the sources, as an analogous to the droop control strategy for overvoltage mitigation in active ENs with high DRES integration [20]. The mathematical formulation of the proposed TDCS is provided in (10) and is graphically illustrated in Fig. 2.

$$Q_{hp,k} = \begin{cases} Q^{max}_{hp,k}, & T^s_{k,out} \le T_{min} \\ Q^{max}_{hp,k} - a\frac{T^s_{k,out} - T_{min}}{T^l_{th} - T_{min}}, & T_{min} < T^s_{k,out} < T^l_{th} \\ Q^{db}_{hp,k}, & T^l_{th} \le T^s_{k,out} \le T^{up}_{th} \\ Q^{db}_{hp,k} - b\frac{T^s_{k,out} - T^{up}_{th}}{T_{max} - T^{up}_{th}}, & T^{up}_{th} < T^s_{k,out} < T_{max} \\ Q^{min}_{hp,k}, & T^s_{k,out} \ge T_{max} \end{cases} \\ \forall k \in \Theta \tag{10}$$

$$a = Q^{max}_{hp,k} - Q^{db}_{hp,k}, \quad \forall k \in \Theta \tag{11}$$

$$b = Q^{db}_{hp,k} - Q^{min}_{hp,k}, \quad \forall k \in \Theta \tag{12}$$

$Q^{min}_{hp,k}$ and $Q^{max}_{hp,k}$ stand for the minimum and the maximum output of the HP in node k. $Q^{db}_{hp,k}$ corresponds to the thermal power generated when the HP operates within the deadband, where no control is activated. a and b are constant parameters for each HP, calculated according to (11) and (12), respectively. T^l_{th} and T^{up}_{th} stand for the lower and upper temperature thresholds for the activation of the TDCS, respectively. T_{min} and T_{max} correspond to the minimum and the maximum permissible nodal supply temperatures.

III. System Under Analysis

The performance of the proposed comprehensive solution is evaluated in the integrated EN and DHN system depicted in Fig. 3. The EN comprises a small-scale LV distribution grid, where multiple PV units are connected. Details regarding the EN configuration can be found in [20].

The examined DHN is part of a real system located in Kozani region, Greece. The DHN is supplied by a slack node which is an ideal thermal generation unit that maintains the temperature and the pressure of the supply subsystem constant and equal to 105 °C and 18 bar, respectively. This slack node can be regarded as a thermal-hydraulic analogous to the slack bus in ENs and is introduced to cover any heat power mismatch of the DHN [10]. The parameters of the DHN pipes are presented in Table I, where D corresponds to the pipe diameter. It is worth mentioning that the number of each pipe corresponds to the number of the *To Node* in

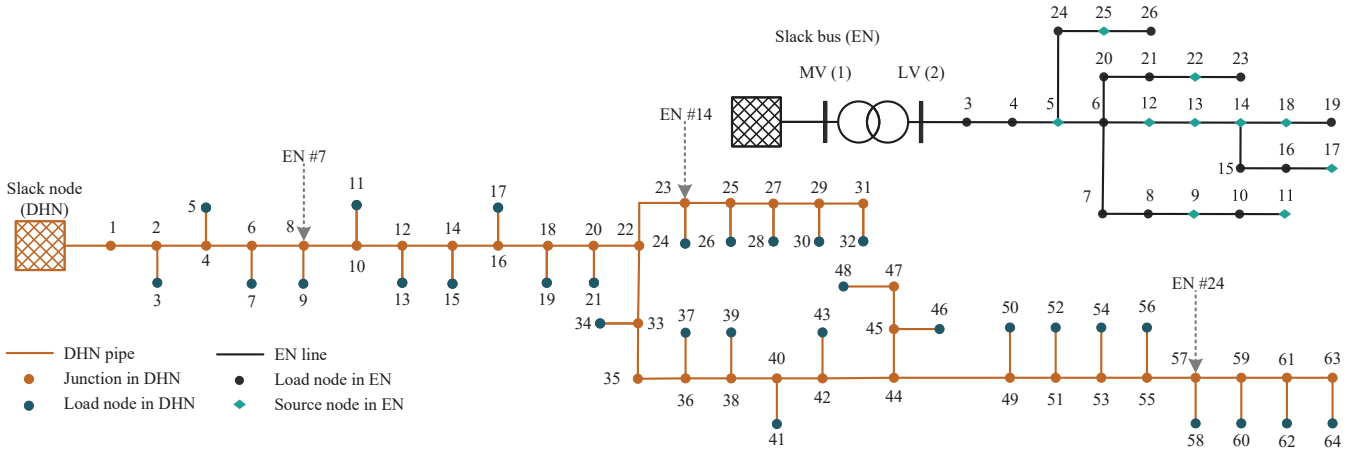

Fig. 3. MES topology consisting of a LV EN and a real DHN.

Table I minus 1. In Table II, the thermal loads connected to the DHN nodes are presented. The heat transfer coefficient λ of the DHN pipes are provided in Table III with respect to D [21]. The ambient temperature T_a is assumed equal to 10 °C, while water is used as heat medium, with specific heat c_p equal to 4182 J/kgK.

As shown in Fig. 3, three high temperature HPs are considered in the examined MES, acting as coupling devices between the EN and the DHN [22]. Considering the operating parameters of the HPs, the COP and the outlet temperature ($T_{o,s}$) are equal to 2.5 and 110 °C, respectively. Finally, the loads outlet temperature ($T_{o,l}$) is set equal to 75 °C.

Eqs. (1)-(12) that mathematically describe the proposed comprehensive solutions are solved in MATLAB [24] using *fsolve*, which is efficient in reaching system solution without depending on the initial condition estimation.

IV. Comparison With *pandapower-pandapipes*

The performance of the developed model for the combined operation of ENs and DHNs is compared with the already existing open-source software packages *pandapower* and *pandapipes*. The validity of each software package has been demonstrated in [18] and [19] through comparisons with other well-established tools. However, it is worth mentioning that there is a difficulty in modeling the return subsystem with the *pandapipes* software, which is dealt properly in the proposed developed model.

The performance of the proposed EN and DHN models is compared against the *pandapower* and *pandapipes* packages, respectively, in terms of voltage, supply temperature, mass flow and thermal losses. In Fig. 4a, the difference in the EN voltages is displayed. Moreover, the difference in the supply temperature and the mass flow of the DHN are shown in Figs. 4b and 4c, respectively. It can be observed that the proposed EN and DHN models have negligible numerical differences with the *pandapower* and *pandapipes* packages, respectively. This is also evident in the calculation of the thermal losses of the supply system which are equal to $13.116 kW_{\text{th}}$, having a negligible difference of $1.727 \cdot 10^{-6}$.

TABLE I
Pipe Parameters of the DHN

From Node	To Node	L (m)	D (mm)	From Node	To Node	L (m)	D (mm)
1	2	4.86	125	33	34	11.22	25
2	3	6.73	25	33	35	10.22	125
2	4	4.90	125	35	36	18.98	65
4	5	10.17	40	36	37	12.41	25
4	6	9.08	125	36	38	6.29	65
6	7	4.49	25	38	39	5.23	25
6	8	12.10	125	38	40	3.64	65
8	9	7.53	25	40	41	9.97	32
8	10	6.42	125	40	42	8.36	65
10	11	7.60	25	42	43	10.55	25
10	12	6.32	125	42	44	18.20	65
12	13	4.87	25	44	45	23.24	40
12	14	9.46	125	45	46	23.51	32
14	15	4.46	25	45	47	9.04	40
14	16	2.98	125	47	48	3.99	25
16	17	10.57	25	44	49	9.17	65
16	18	2.70	125	49	50	15.23	25
18	19	9.55	25	49	51	3.86	65
18	20	6.28	125	51	52	9.42	25
20	21	4.05	25	51	53	21.35	65
20	22	11.29	125	53	54	12.18	25
22	23	28.57	50	53	55	4.77	65
23	24	6.17	32	55	56	6.31	25
23	25	21.07	50	55	57	5.29	65
25	26	4.76	25	57	58	29.25	25
25	27	8.04	50	57	59	16.23	65
27	28	9.71	25	59	60	6.65	25
27	29	14.63	50	59	61	14.59	65
29	30	7.84	25	61	62	3.59	25
29	31	18.83	50	61	63	10.18	65
31	32	9.19	25	63	64	4.54	25
22	33	3.04	125	–	–	–	–

TABLE II
Rated Thermal Power Consumption

Thermal Load	Nodes
23.24 (kW_{th})	19,26
46.48 (kW_{th})	3,7,9,11,13,15,17,21,28,30,32,34,37 39,43,46,48,50,52,54,56,58,60,62,64
69.72 (kW_{th})	24,41
116.20 (kW_{th})	5

TABLE III
Heat Transfer Coefficient in Relation to Pipe Diameter

D (mm)	25	32	40	50	65	125
λ (W_{th}/m·K)	0.18	0.189	0.21	0.219	0.236	0.321

V. Assessment Of The Proposed TDCS Integration

In this work, a detailed modeling approach is developed and presented for the steady-state integrated operation of ENs and DHNs, where HPs are employed. The model is further enhanced through the implementation of a TDCS introduced in the operation of the HPs. Specifically, as the HPs installation affects the temperature mainly in the supply subsystem, (10) is used to control the output HP thermal power, which is injected to the DHN. Higher value of the HP thermal power leads to higher temperature across the DHN, starting from the connection node. In (10), T_{min}, T^l_{th},

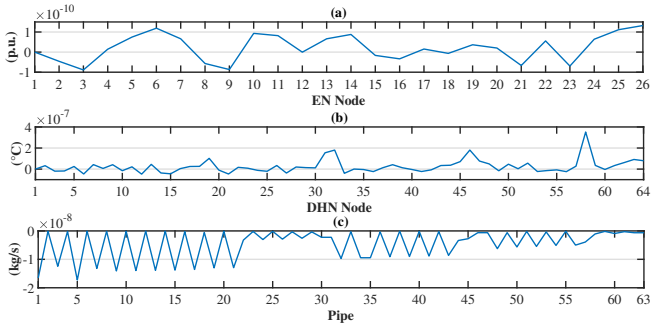

Fig. 4. Comparison between the operation of the proposed model and the open-source software. Calculated difference in the magnitude of (a) voltage, (b) temperature, and (c) mass flow.

T_{th}^{up} and T_{max} are set equal to 102.375 °C, 104.475 °C, 105.525 °C and 107.625 °C, respectively, which correspond to deviation in percentage with respect to the temperature in the slack node equal to -2.5 %, -0.5 %, +0.5 %, and +2.5 %, respectively. The temperature values are selected considering the temperature level of the supply subsystem, which is equal to 105 °C in the DHN under study. $Q_{hp,k}^{min}$, $Q_{hp,k}^{db}$ and $Q_{hp,k}^{max}$ are set equal to 50 %, 75 % and 100 % of the HP rated thermal output, respectively.

To study the effectiveness of the proposed technique, the following three scenarios are examined: (a) baseline scenario where the EN and DHN operate with no HP connection (Scenario 0), (b) combined operation of EN and DHN with HPs installed in Nodes 8, 23 and 57 of the DHN, as depicted in Fig. 3 (Scenario 1), and (c) combined operation of EN and DHN, as in Scenario 1, enhanced by the implementation of the proposed TDCS to the HPs (Scenario 2).

The HPs thermal output for each scenario is presented in Table IV. Assuming that the rated power of the HPs installed is equal to 174.3 kW_{th}, they are set to operate at 75 % in Scenario 1. This leads to increased temperature in the supply subsystem starting from the nodes where the HPs are connected, i.e, Nodes 8, 23 and 57, as presented in Fig. 5. Specifically, in Node 57, the temperature is equal to 104.749 °C in Scenario 0, while it is increased to 108.349 °C in Scenario 1. Thus, as the temperature exceeds T_{max}, the TDCS is activated in Scenario 2, leading to a decrease in the temperature, which becomes 107.366 °C. This is a result of the corresponding HP thermal power which is decreased, as seen in Table IV, due to the activation of the TDCS according to (10). Moreover, the temperature in Node 8 and 23 is successfully decreased, with the first one operating at the third region of (10) (temperature equal to 105.500 °C) and the second operating at the fourth (temperature equal to 107.105 °C).

Regarding the temperature in the whole DHN, Fig. 5 illustrates the temperature variation in the supply subsystem across the two DHN branches, as shown in Fig. 3. It can be observed that in Scenario 0 across the supply subsystem there is a temperature reduction due to thermal losses, in both the DHN branches, starting from Node 1. The same result can be extracted also for the return subsystem, i.e., the temperature reduction from node to node, but in the opposite direction, as shown in Fig. 6. Nevertheless, the temperature deviations in the return subsystem caused by the combined operation of EN and DHN are very small even in Scenario 2.

The developed model can also calculate the mass flow in the pipes of the DHN, presented in Fig. 7. It can be observed

TABLE IV
GENERATED HP THERMAL POWER (kW_{TH})

	Scenario 0	Scenario 1	Scenario 2
Node 8	0	130.725	130.725
Node 23	0	130.725	97.944
Node 57	0	130.725	92.528

TABLE V
LOSSES ACROSS THE NETWORKS

	Scenario 0	Scenario 1	Scenario 2
EN Losses	11.32 kW_{el}	6.37 kW_{el}	3.60 kW_{el}
DHN Losses	22.09 kW_{th}	22.26 kW_{th}	22.22 kW_{th}

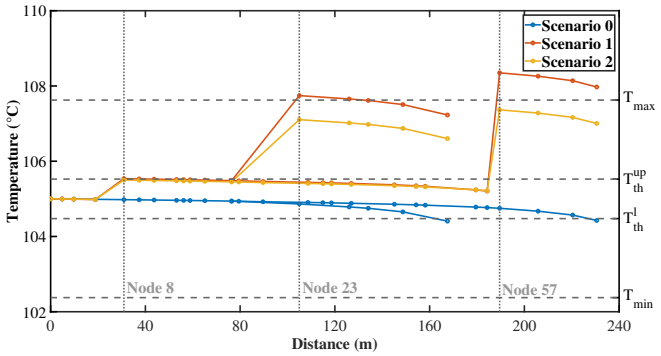

Fig. 5. Node temperature in the supply subsystem.

that with the HPs installation, the mass flow from the slack node is reduced, justifying that the generated power from DRES is exploited locally, leading to decreased input from the rest of the network. In fact, in Scenario 2 when the HPs output is reduced to control the node temperature, the mass flow is increased following the corresponding temperature decrease. However, in Table V it can be observed that the thermal losses of the DHN are increased with the installation of the HPs when examining Scenario 1, as a result of the temperature increase. Both EN and DHN losses are decreased in Scenario 2 proving the effectiveness of the TDCS operation. Note that the variations in the DHN losses are small due to the system configuration, i.e., the relatively short length of the pipes, accompanied by the pipe diameter and the operational temperature level.

Regarding EN, the integrated operation EN and DHN leads to overvoltage mitigation, as shown in Fig. 8. In Scenario 0, the node voltage exceeds the upper limit, which is equal to 1.1 p.u. for LV distribution grids [23]. This is a result of the high PV penetration, which is dealt properly in Scenarios 1 and 2. Finally, through the analysis, the TDCS seems to be effective in reducing the EN losses, as observed in Table V.

VI. CONCLUSIONS

In this paper, a detailed model is presented dealing with the steady-state integrated operation of ENs and DHNs. Results by the proposed model are compared to those by the existing software packages, *pandapower* and *pandapipes*, achieving high value of accuracy. The developed model is enhanced by the integration of a TDCS in the operation of the HPs, which are used as coupling devices. It is concluded that the proposed TDCS is effective in managing the temperature in the supply subsystem, which is increased due to the HPs installation. Moreover, it is concluded that both with and without the TDCS implementation, the overvoltages are mitigated properly and the EN losses are decreased. Thus, the integrated operation of ENs and DHNs leads to higher exploitation of

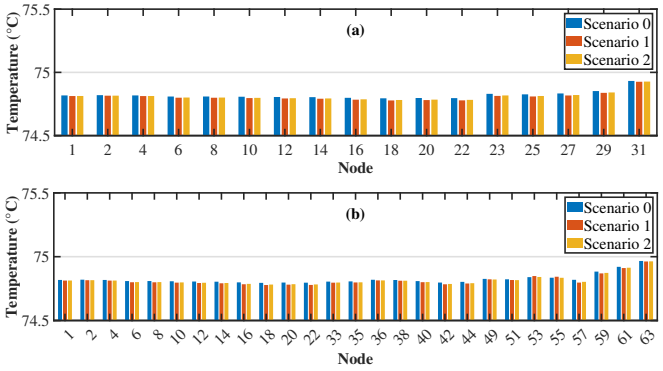

Fig. 6. Node temperature in the return subsystem. (a) Upper branch of DHN, and (b) Lower branch of DHN.

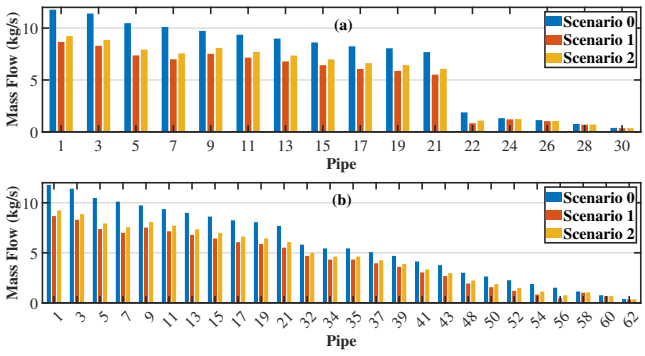

Fig. 7. Mass flow within the pipes. (a) Upper branch of DHN, and (b) Lower branch of DHN.

the DRES generation, respecting the temperature limits in DHN when enhanced by the proposed TDCS.

As future work, at first, the introduction of time delay is proposed to consider the dynamic energy propagation along the DHN. The model will be enriched to be capable of implementing cost analysis. Moreover, the proposed model will be further enhanced by including the unbalances that may occur in the operation of the EN. Such a detailed tool including all the above-mentioned features, could be a valuable asset for the relevant stakeholders, i.e., the system operators, to simulate and plan the combined operation of the MESs.

ACKNOWLEDGMENT

The authors would like to thank the Municipal Enterprise for Water Supply, Sewerage and District Heating of Kozani, Greece, for providing the data corresponding to the DHN used for the analysis in the framework of this work.

REFERENCES

[1] "'Fit for 55': delivering the EU's 2030 Climate Target on the way to climate neutrality," Brussels, 14.7.2021, COM(2021) 550 final.
[2] "A Clean Planet for all: A European strategic long-term vision for a prosperous, modern, competitive and climate neutral economy," Brussels, 28.11.2018, COM(2018) 773 final.
[3] R. Bacher, E. Peirano, M. Nigris, et al., "Vision 2050, Integrating Smart Networks for the Energy Transition: Serving Society and Protecting the Environment," Plan Innovate Engage, 2019.
[4] "Powering a climate-neutral economy: An EU Strategy for Energy System Integration," Brussels, 8.7.2020, COM(2020) 299 final.
[5] P. Mancarella, "MES (multi-energy systems): An overview of concepts and evaluation models," Energy, vol. 65, no. 2, pp. 1–17, 2014.
[6] X. Li, W.Li, R. Zhang, et al., "Collaborative scheduling and flexibility assessment of integrated electricity and district heating systems utilizing thermal inertia of district heating network and aggregated buildings," *Applied Energy*, vol. 258, pp. 114021, Jan. 2020.
[7] R. Tonkoski, D. Turcotte, and T. H. M. El-Fouly, "Impact of high PV penetration on voltage profiles in residential neighborhoods," *IEEE Trans. Sustain. Energy*, vol. 3, no. 3, pp. 518–527, Jul. 2012.

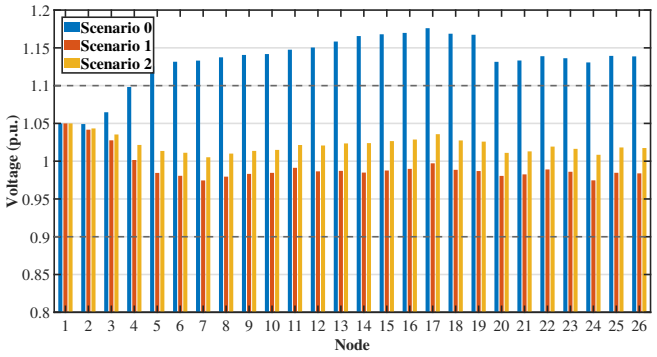

Fig. 8. Node voltage in the EN.

[8] Y. Jiang, C. Wan, A. Botterud, Y. Song and S. Xia, "Exploiting Flexibility of District Heating Networks in Combined Heat and Power Dispatch," *IEEE Trans. Sustain. Energy*, vol. 11, no. 4, pp. 2174-2188, Oct. 2020.
[9] M. Geidl, and G. Anderson, "Optimal Power Flow of Multiple Energy Carriers," *IEEE Trans. Power Syst.*, vol. 22, no. 1, pp. 145–155, Feb. 2007.
[10] X. Liu, J. Wu, N. Jenkins, and A. Bagdanavicius, "Combined analysis of electricity and heat networks," *Applied Energy*, vol. 162, pp. 1238–1250, 2016.
[11] S. Huang, W. Tang, Q. Wu and C. Li, "Network constrained economic dispatch of integrated heat and electricity systems through mixed integer conic programming," *Energy*, vol. 179, pp. 464–474,2019.
[12] J. Chen, F. Li, H. Li, et al., "Novel dynamic equivalent circuit model of integrated energy systems," *Energy*, vol. 262, Part A, pp. 125266, Jan. 2023.
[13] Z. Chen, J. Liu, and X. Liu, "GPU accelerated power flow calculation of integrated electricity and heat system with component-oriented modeling of district heating network," *Applied Energy*, vol. 305, pp. 117832, Jan. 2022.
[14] W. Zheng, Y. Hou and Z. Li, "A Dynamic Equivalent Model for District Heating Networks: Formulation, Existence and Application in Distributed Electricity-Heat Operation," *IEEE Trans. Smart Grid*, vol. 12, no. 3, pp. 2685–2695, May 2021.
[15] J. E. Feghali, G. Sandou, H. Guéguen, et al., "Electrical Grid Flexibility via Heat Pump and Thermal Storage Control," *IFAC-PapersOnLine*, vol. 55, Issue 11, pp. 84–89, 2022.
[16] T. Lan, K. Strunz, "Droop control for district heating networks: Solution for temperature control of multi-energy system with renewable power supply," *Int. J. Electr. Power Energy Syst.*, vol. 146, pp. 108663, Mar. 2023.
[17] S. A. Vomva, G. C. Kryonidis, A. I. Nousdilis, G. C. Christoforidis and G. K. Papagiannis, "Integrated Operation of Droop Controlled Electrical Networks with District Heating Networks," *2022 2nd SyNERGY MED*, Thessaloniki, Greece, 2022, pp. 1–6.
[18] L. Thurner, A. Scheidler, F. Schäfer et al, "pandapower - an Open Source Python Tool for Convenient Modeling, Analysis and Optimization of Electric Power Systems," *IEEE Trans. Power Syst.*, vol. 33, no. 6, pp. 6510–6521, Nov. 2018.
[19] D. Lohmeier, D. Cronbach, S.R. Drauz, M. Braun, and T.M. Kneiske, "Pandapipes: An Open-Source Piping Grid Calculation Package for Multi-Energy Grid Simulations," *Sustainability*, vol. 12, no. 23, pp. 9899, 2020.
[20] G. C. Kryonidis, E. O. Kontis, A. I. Chrysochos, C. S. Demoulias, and G. K. Papagiannis, "A coordinated droop control strategy for overvoltage mitigation in active distribution networks," *IEEE Trans. Smart Grid*, vol. 9, no. 5, pp. 5260—5270, Sep. 2018.
[21] M. Pirouti, "Modelling and Analysis of a District Heating Network," PhD Thesis, Cardiff University, Feb. 2013.
[22] J. Barco-Burgos, J.C. Bruno, U. Eicker, A.L. Saldaña-Robles and V. Alcántar-Camarena, "Review on the integration of high-temperature heat pumps in district heating and cooling networks," *Energy*, vol. 239, Part E, pp. 122378, Jan. 2022.
[23] Voltage Characteristics of Electricity Supplied by Public Distribution Networks, BS EN Standard 50160, 2010.
[24] MATLAB 2018b, The MathWorks, Inc., Natick, Massachusetts, United States, 2018.